3 ATF OVERVIEW

3.1 Introduction:

The Brookhaven National Laboratory Accelerator Test Facility (ATF) [5-6] has been established to provide high-brightness electron beams and high-power, short-pulse laser beams for users to enable investigations into electron-laser interactions as well as experiments into the physics of beams.

The ATF has three beam lines dedicated to various experiments, which can run one at a time. In many of these experiments, the electrons either transfer energy to the laser's electromagnetic field or vice versa.

The ATF's electron accelerator system consists of a radio frequency (RF) photo cathode electron gun, two SLAC type Linear Accelerator (Linac) sections and three experiment beam lines. The laser system includes a gigawatt peak power Nd:YAG laser, which is at 1064 nm wavelength and 15 ps pulse length, and a gigawatt CO2 laser, which is at 10.6 μm wavelength and 200 ps pulse length. The RF gun is a 1.6 cell photo-cathode RF electron gun with magnesium cathode, operating at 2856 MHz. The Linac is also operating at the same frequency. The facility can deliver electron beams with typically 1nC charge and 1 to 8 ps pulse length, of the order of 3 μrad normalized rms emittance up to an energy of about 70 MeV. The ATF block-diagram is shown in Figure 3-1.

The 1064 nm Nd:YAG laser is used to produce the photoelectrons in the electron gun and, at the same time, switch a short pulse out of the CO2 laser. In this way this laser provides the necessary high-precision synchronization between the electron beam and the CO2 laser. There are two master clocks in the system. One is the RF high-stability crystal-controlled reference oscillator, (see Figure 3-1) and the other is the mode-locked Nd:YAG oscillator, which provides the timing of the lasers. Both run at a frequency of 81.6 MHz. The phase of the laser oscillator is locked to the RF reference by a phase-lock control circuit. Various time delays can be generated by electronic delay generators, but

the high-precision timing is determined by the phase-locked laser oscillators and RF reference oscillator.

The magnesium cathode is illuminated by the frequency-quadrupled (266nm UV) Nd:YAG laser and the electrons are accelerated up to 4.5 MeV energy at the end of the RF gun. Then electrons are accelerated by the two section of the Linac and reach energies up several tens of MeV's, depending on the experiment.

As can be seen in Figure 3-1, the gun and the Linac are powered by two separate klystrons. The phase of these power sources relative to the reference can be independently adjusted by electronic phase shifters, and the amplitude can be set by variable attenuators. The set point of these elements is controlled by the ATF's control computer. There is also a mechanical waveguide phase shifter between the two Linac sections to adjust the relative phase of these two sections.

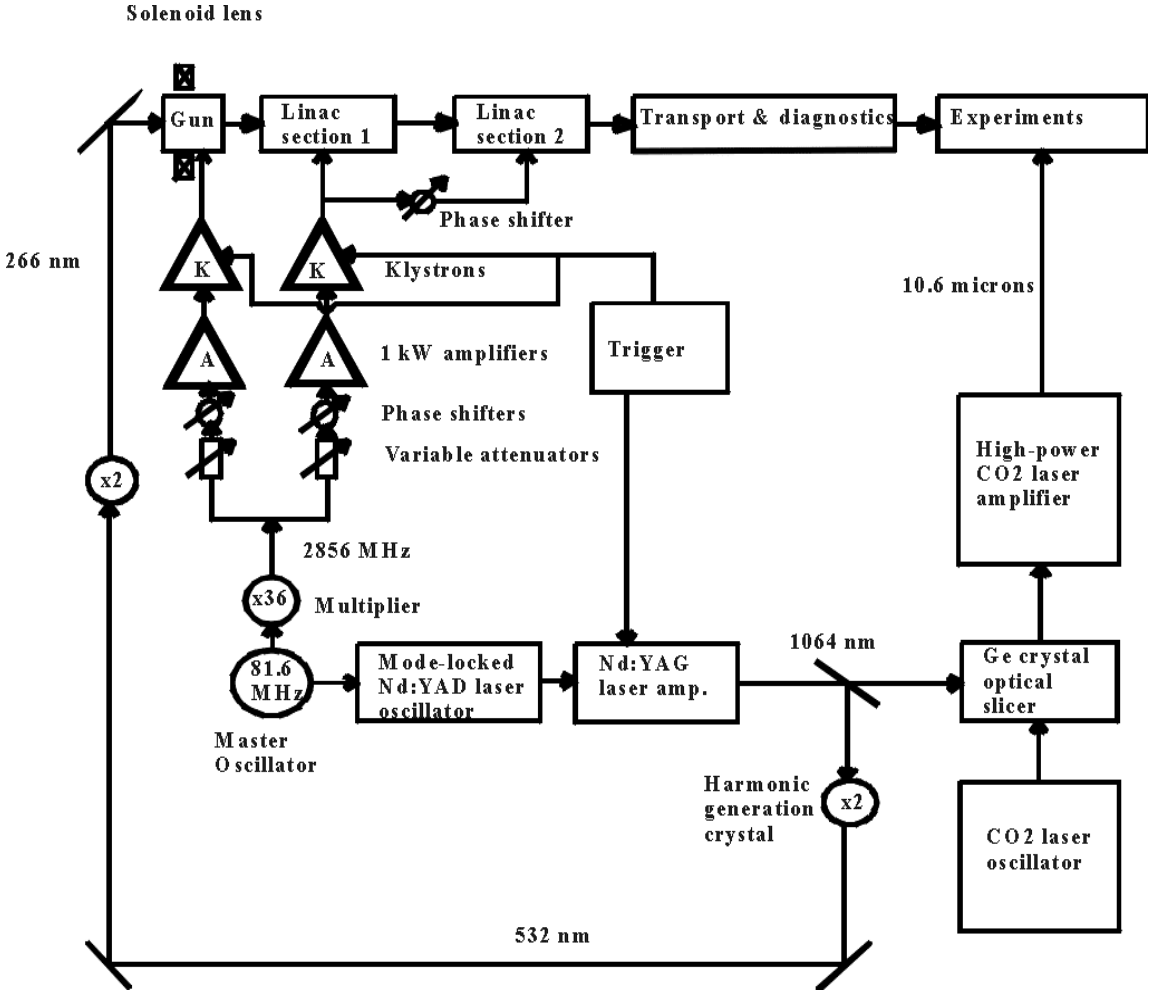

Figure 3-1 Block Diagram of ATF System

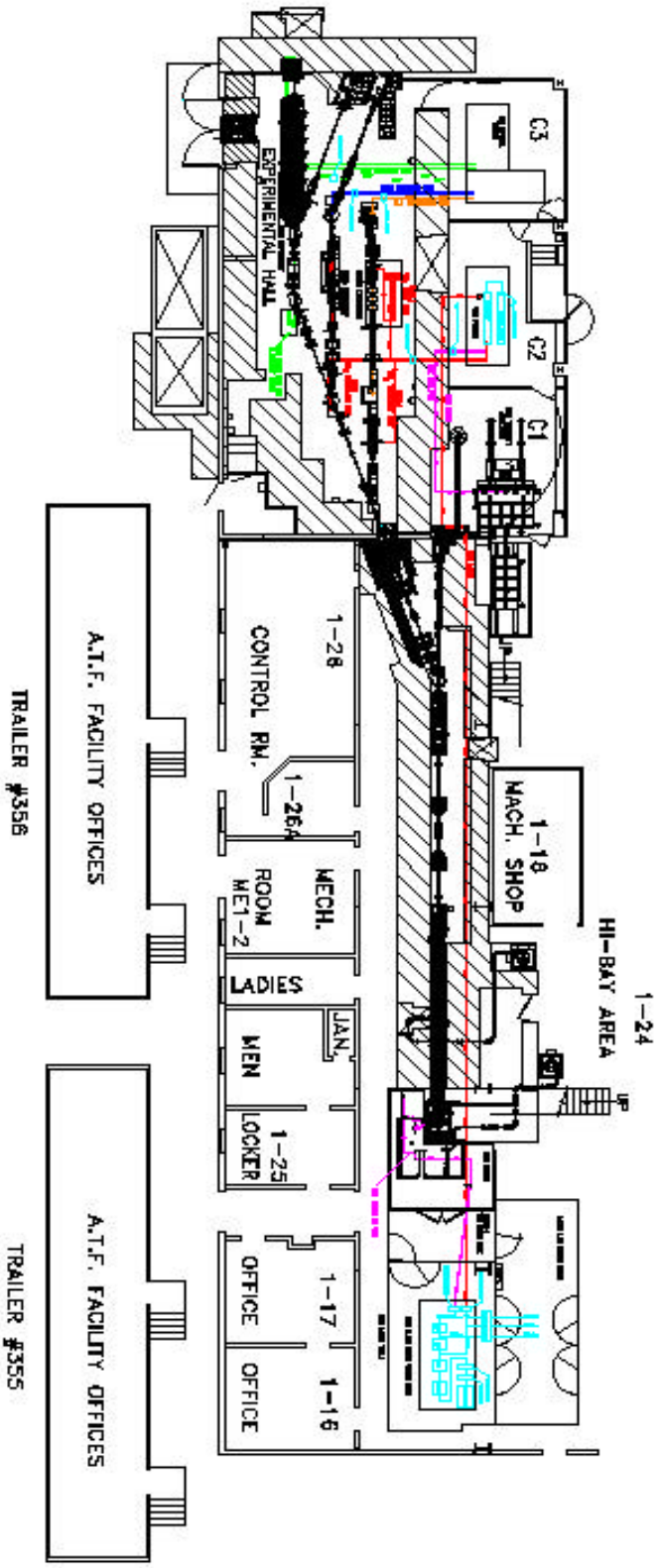

Figure 3-2 ATF Building Overview

Figure 3-2 shows an overview of the Accelerator Test Facility. On the right (South) we have the Nd:YAG laser and the injection system. The electron beam is accelerated towards north (left in the figure) by the Linac, and then transported by the high energy line (H line and F line). In these lines we have electron beam diagnostic devices, where we can measure the emittance and pulse length of the beam. These measurements will be explained later on in more detail. Finally the beam reaches to the experimental area, where it may be switched into any one of three independent beam lines.

Room C1 contains the terawatt CO_2 laser, which is currently under commissioning. Room C2 houses the gigawatt CO_2 laser room. Optical analysis of the FEL is done in room C3 (nicknamed the FEL room)

3.2 The Nd:YAG Laser System

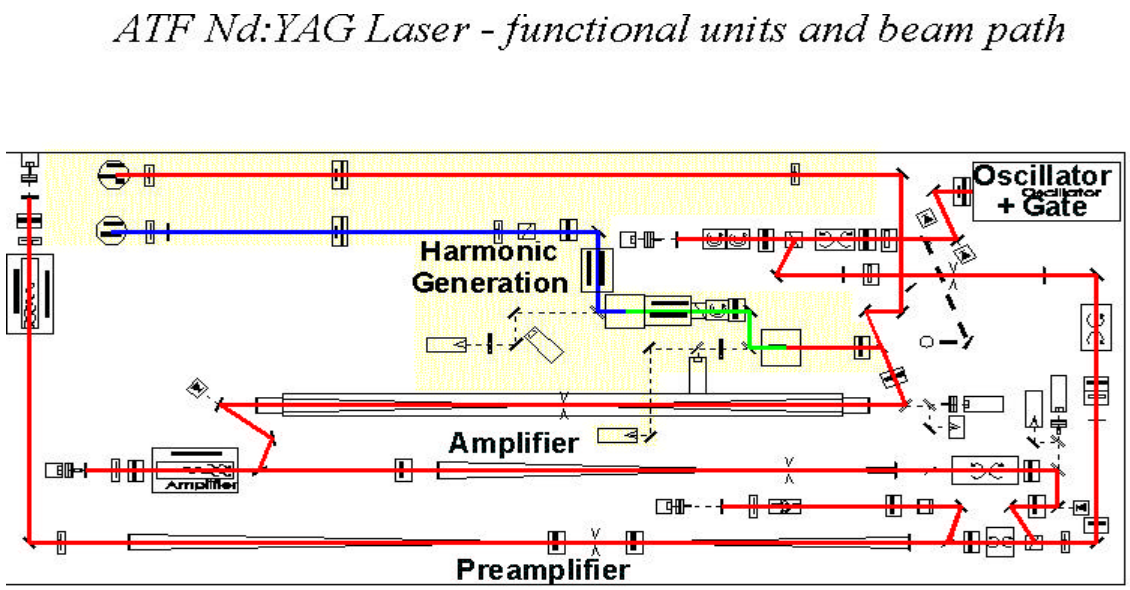

Figure 3-3 YAG System Layout

The Nd:YAG Laser is located in a class 1000 clean room (the YAG room) upstream of the electron gun. The Nd:YAG laser is operated in a linear amplifier mode, capable of producing a unique pulse train. The schematic diagram of the YAG system is shown in Figure 3-3. The red line represents the 1064 nm infrared, green represents the 532 nm green light and blue represents the 266 nm UV light. The energy of the YAG

laser is about 30 mJ with a pulse length of 15 ps. The YAG is split and 20 mJ is sent to the CO_2 system to produce slicing. Then the remaining part of the YAG laser is doubled and then quadrupled to obtain 266 nm UV light. The UV light is transported to the electron gun in the gun hutch room in about 15 m of enclosed transport line. The energy of the UV is about 0.2 mJ of which is ~1/3, ~1/5 of it available in a 3 mm beam size on the cathode. The FWHM pulse length of the beam is about 8 ps. In the gun hutch the beam is focused in the gun cathode to produce electrons. The optics are shown in Figure 3-4. A part of the beam is split before the cathode to form the image of the cathode position. This allows us to get information about the laser properties at the cathode such as beam size, intensity and so on. The second surface reflection from the beam splitter is also sent to a joulemeter, thus providing a reference energy reading for the laser. Various laser parameters are under computer control. These include power, and vertical and horizontal position. The diagnostics allow us to monitor remote-controlled changes of these parameters.

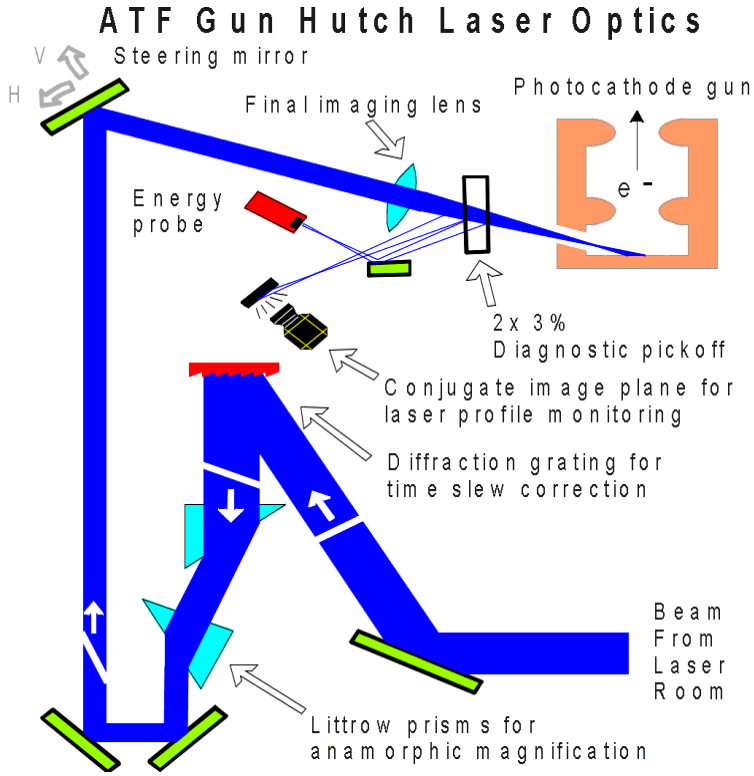

Figure 3-4 Gun Hutch Optics.

3.3 The Electron RF Gun

The electron source of the ATF is called a photo-cathode RF gun, or photoinjector. In this type of gun short bunches of electrons are produced by UV laser pulses incident on a photo-cathode. The photo-cathode is located on a back wall of an RF cavity. High power microwave (up to 6 MW) drive the cavity to a high electric field.

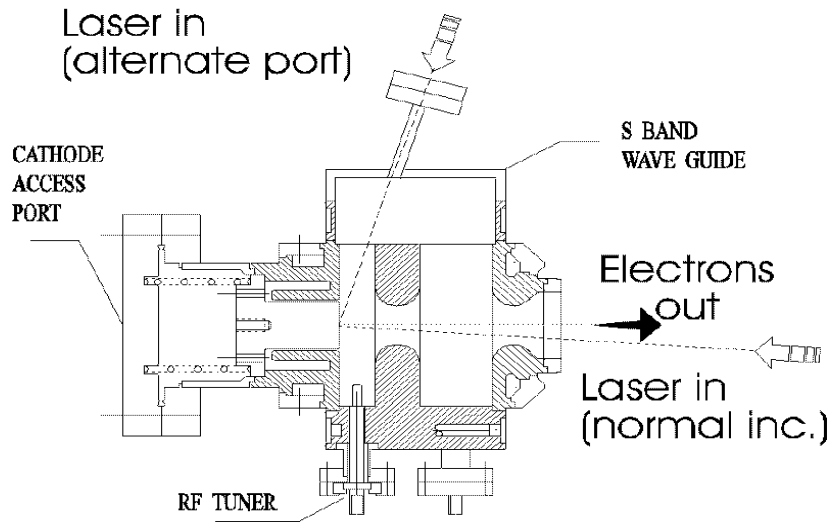

Figure 3-5 Drawing of the Photocathode RF gun, cut along the beam axis.

The schematic diagram of the RF gun is shown in Figure 3-5. The reason for operating the gun at a high accelerating field is to make the electrons relativistic in a very short distance. The motivation for a rapid acceleration is to minimize the time the electron bunch is affected by strong space-charge forces, thus minimizing phase-space distortions. In addition, the high electric field on the cathode allows a large current density. At a low field the current is limited by repulsion of electrons by the space-charge induced field of the earlier electrons. To get a high charge at reasonable laser intensity, the quantum efficiency of the cathode should be high. A high electric field helps to increase the quantum efficiency by the Schottky effect [7]. The current density that can be achieved ranges from 10 to 100000 A/cm^2. This current density is much larger than the current density that may be achieved by thermionic guns (about 10 A/cm^2). Brightness is proportional to the current density thus a photoinjector is a much higher brightness device than a thermionic gun. With a photoinjector it is possible to obtain a peak current of 100 A or more with a normalized emittance of 3 μrad.

RF wise, the ATF RF gun is a resonant π-mode 1.6 cell cavity operating at the frequency of 2856 MHz. Currently a magnesium cathode is being used, while previously a copper cathode has been used.

RF frequency (MHz)	2856
Cathode cell length (cm)	2.625
Second cell length (cm)	5.23
Cell diameter (cm)	8.31
Radius of aperture (cm)	1.25
Field on cathode (MV/m)	100
Peak field on wall (MV/m)	106
RF power (MW)	5.9
Cavity Q	12000
Effective shunt impedance (MΩ/m)	57

Table 3-1 Gun parameters

In Table 3-1the gun parameters are shown and Figure 3-6 is the photo of the gun.

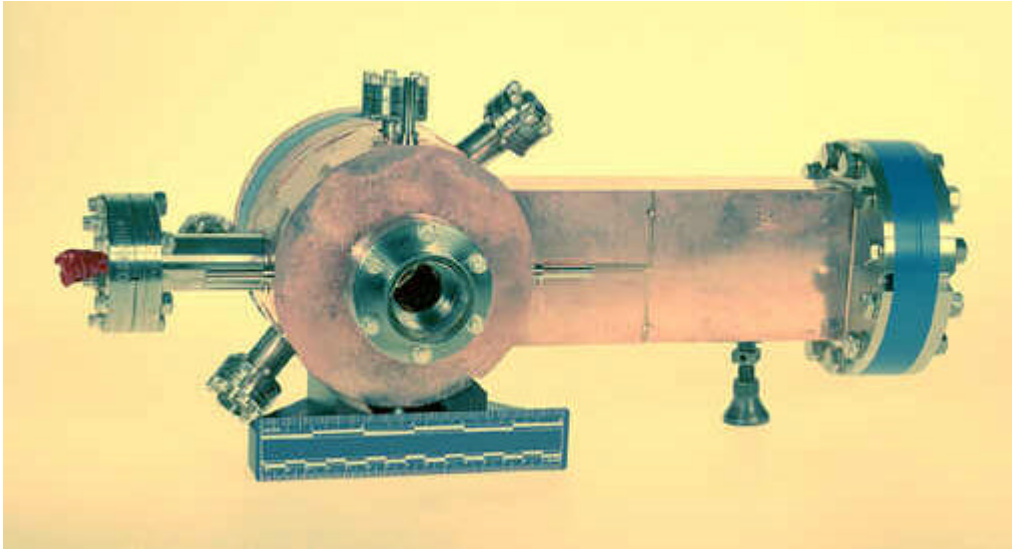

Figure 3-6 Photograph of the ATF photocathode RF Gun

We have a solenoid lens around the gun, which is used for emittance compensation. More detailed information about the emittance compensation can be obtained from references [8-10].

The RF forward power and phase can be controlled remotely by the ATF VAX computer system. In the context of the photoinjector, the RF phase is the relative timing of the RF voltage with respect to the Nd:YAG laser. As we change the RF phase the charge extracted from the cathode changes with the magnitude of the field. We define the phase of maximum charge as 90^0. Usually we operate at a phase of 60^0, which produces a good emittance with no bunch compression [11-12].

3.4 The LINAC and The High Energy Transport Line

ATF Linear Accelerator is a traveling wave SLAC type of accelerator, which consists of two sections.

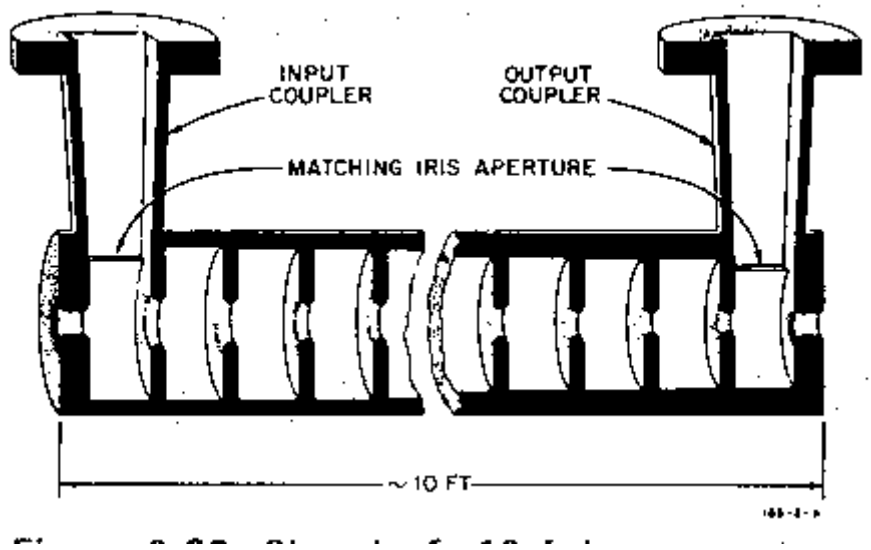

Figure 3-7 SLAC Type Linac Structure

These sections have been made by the Institute of High Energy Physics in Beijing, China, following the design of the Linac structures developed at the Stanford Linear Accelerator Center (SLAC). The SLAC accelerator structure is shown in Figure 3-7. Each section of the Linac is 3 m long and operates at a frequency of 2856 MHz. The Linac is driven by a high power microwave tube called a klystron. The klystron used at the ATF can go up in power to about 28 MW. With this available microwave power distributed to both sections, it is possible to accelerate the beam by about 68 MeV, thus obtain up to 72 MeV electrons (with about 4.5 MeV coming from the gun). Between the two sections there is a mechanical phase shifter. In normal operating conditions, this phase shifter is set for equal phase (relative to the electron bunch) in both sections for minimizing the energy spread of the beam. In another application it is used for bunch length measurement of the electron beam [10]. In Figure 3-8, ATF injection, the Linac and the high-energy transport line are shown. This figure is highly schematic. Actually it is a drawing taken from the computer control software. (In this figure, the beam goes from right to left and top to bottom). On the top line we can see the gun, solenoid and monitor named LPOP-UP 1, which is also a Faraday cup [13].

The ATF beam diagnostics include beam profile and position monitors that produce an image of the beam on a video monitor [13]. The beam image is produced by a

phosphor screen (or some other device that converts beam impact to visible radiation). The optical radiation from the screen is imaged by a CCD (Charge Coupled Device) camera. A 'Frame Grabber', a piece of hardware that converts the video signal from the CCD camera to a digital matrix, captures the information from the camera. ATF frame grabber can analyze the intensity and beam size properties. The Faraday cup is essentially an isolated electrode, which is designed to stop and capture the beam charge. Using an oscilloscope we can measure the current across the Faraday cup when an electron bunch hit. The scope's numerical analysis hardware can calculate the area of the current signal, that is the charge. Thus LPOP-UP 1 monitor is where we measure the charge coming out of the RF gun. In addition, we have two horizontal and vertical steering magnets to adjust the position and the angle of the beam at the entrance of the Linac. We have some steering magnets inside the Linac to get better alignment of the beam through the length of the Linac. The second line in Figure 3-8 shows the Linac.

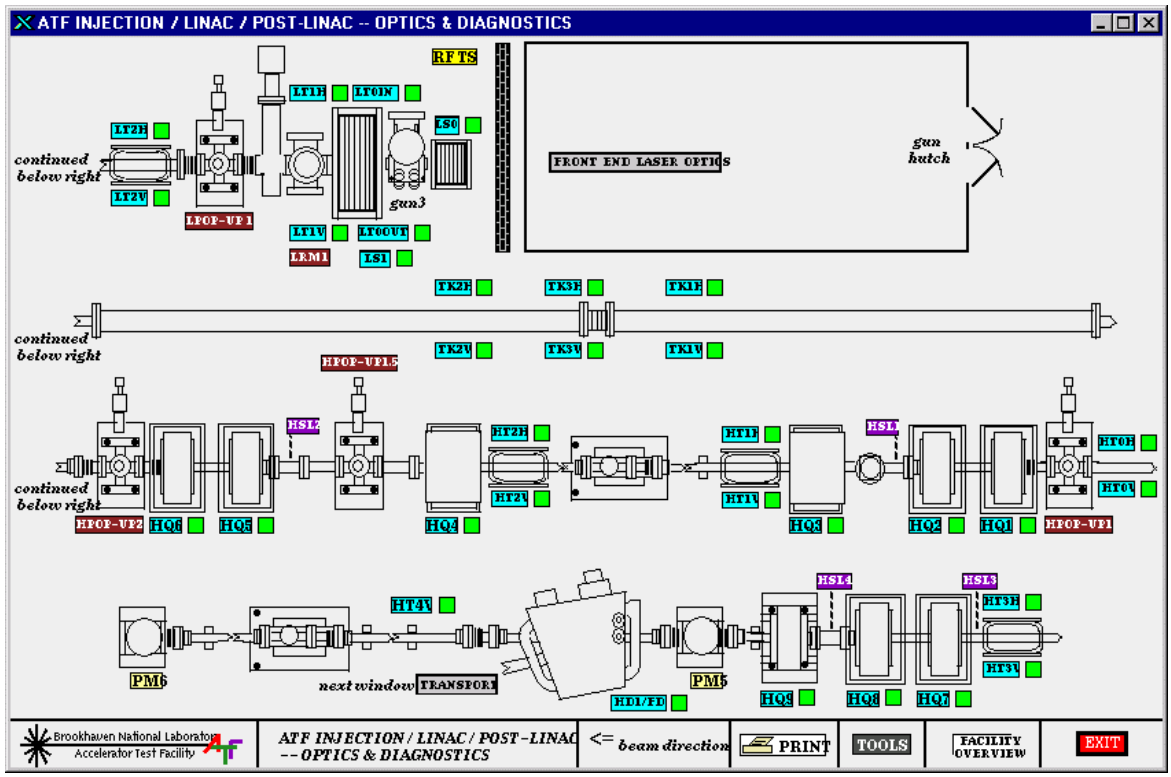

Figure 3-8 Control-computer display showing elements of the ATF Injection, Linac and High Energy Transport Systems.

3.5 The High Energy Transport Line and the F Line

High Energy (H line) line up to the first dipole magnet. The H line comprises nine quadrupole magnets named HQ1 through HQ9, trim magnets, diagnostics and vacuum equipment. The purpose of the quadrupoles is to confine the electron beam to the beam line. The trim magnets are used to control the trajectory. As shown in Figure 3-8, the diagnostics include the profile / position monitors named HPOP-UP 1, HPOP-UP 1.5 and HPOP-UP 2. These monitors image the beam profile at these locations. Following the H line electrons are bent 20 ^{0} horizontally by a dipole magnet, which is called HD1. From this position the transport line is called the F line. The dipole magnet acts as an energy spectrometer due to fact that electrons are bent in inverse relation to their energy. Downstream of the dipole, at the location of the High energy Slit (HES) we can correlate the horizontal beam size to the energy spread of the electron beam. The location of the HES is characterized by a large 'analyzing power', that is a large value of the ratio dispersion function over horizontal betatron size. Before we start the experiment we simulate the transport line using either the TRANSPORT [14] or MAD [15] program for a certain energy, which is specific for the experiment. Then, by varying the quadrupole magnet strengths we optimize the beam sizes and the dispersion for overall transport line. The dispersion is defined as

$$x \equiv D(p,s)\frac{\Delta P}{P_0} \qquad \text{Eqn 3-1}$$

where x is the transverse displacement, s is the longitudinal coordinate along the ideal trajectory, P is the momentum and $D(p,s)$ is the dispersion function.

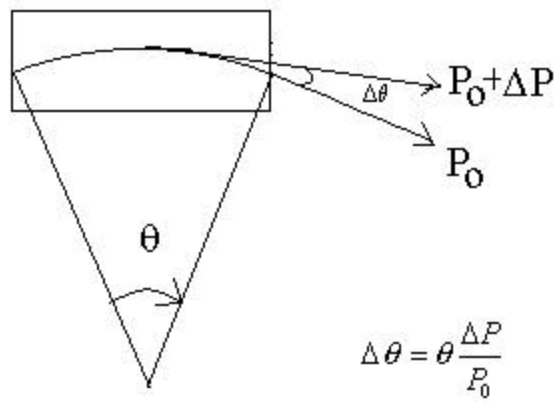

Figure 3-9 Dispersion due to a dipole magnet. θ is the bend angle for an electron with momentum P_0, Δθ is the change in the bend angle due to a momentum offset ΔP.

Following the F line we have another -20^0 dipole, which bends the beam into the original direction. The simulation programs calculate and optimize the dispersion and betatron size of the beam, thus avoid large transverse beam size in the F line. The programs also solve for the quadrupole strengths produce a vanishing dispersion and dispersion derivative at the exit of the F line. We start from these calculated quadrupole magnet strength values and then fine-tune the values by observing the beam profile monitors. At the HPOP-UP 1 monitor we adjust the solenoid lens to get a reasonably small and round beam. Then we check the beam at HPOP-UP 2 monitor and slightly adjust the HQ1,2,3 quadrupole magnets to get the beam as small as possible. At these monitors we also check the roundness of the beam. Sometimes electron beam does not go through the centers of the quadrupole magnets. This may cause aberrations in the beam profile and also deflect the electron beam from the axis when the quadrupole current is being changed. The technique to check for such misalignment and correct it is called 'steering'. When we check for steering we gradually change the quadrupole strength and look at the beam position downstream of the quadrupole magnet. If the beam passes through the center of the quadrupole magnet then as we change the strength it should not steer (move) the beam. However if it does not pass through the center then it would steer the beam. In this case we use trim magnets (correctors) to center the beam in the quadrupole.

Another diagnostic on the H line is the BPM5 monitor. In a typical operation we use this monitor to measure the emittance. The emittance measurement will be described later.

The high analyzing power at the HES allows us to measure the energy spread. Most of the energy spread is introduced by the Linac. Since the beam has a finite bunch length, the time dependence of the accelerating voltage will introduce a spread in acceleration. As shown in Figure 3-10, the projection of the beam on the vertical axis represents the energy spread. Therefore the energy spread changes with the RF waveform relative to the electron beam position, or the Linac phase. This phase determines the timing of the Linac with respect to the beam. As with other parameters, we have remote control of the Linac phase. Beam monitor FPOP-UP 1 is located near the HES. We observe the beam size at FPOP-UP 1 monitor (see Figure 3-11) as we change the phase until we achieve the minimum horizontal beam size, which represents the minimum energy spread. This corresponds to the crest of the Linac voltage. After the FPOP-UP 1 monitor we have the High Energy Slit, which can be used to limit the energy spread of the beam. There is also a camera looking at this HES so that we can see the edges of the beam on both sides. The slit is vertical and both jaws can be moved independently by a very sensitive stepper motor. 10000 steps for each jaw, which is about 3 mm slit opening, corresponds to 0.6 % energy spread.

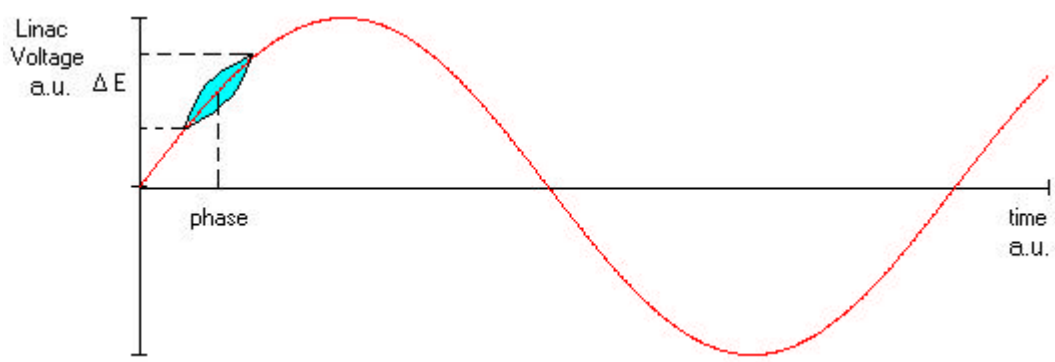

Figure 3-10 Linac RF Voltage waveform, showing (in blue) the electron bunch (distributed in energy and phase following the ‘chirp’ induced by the RF waveform.

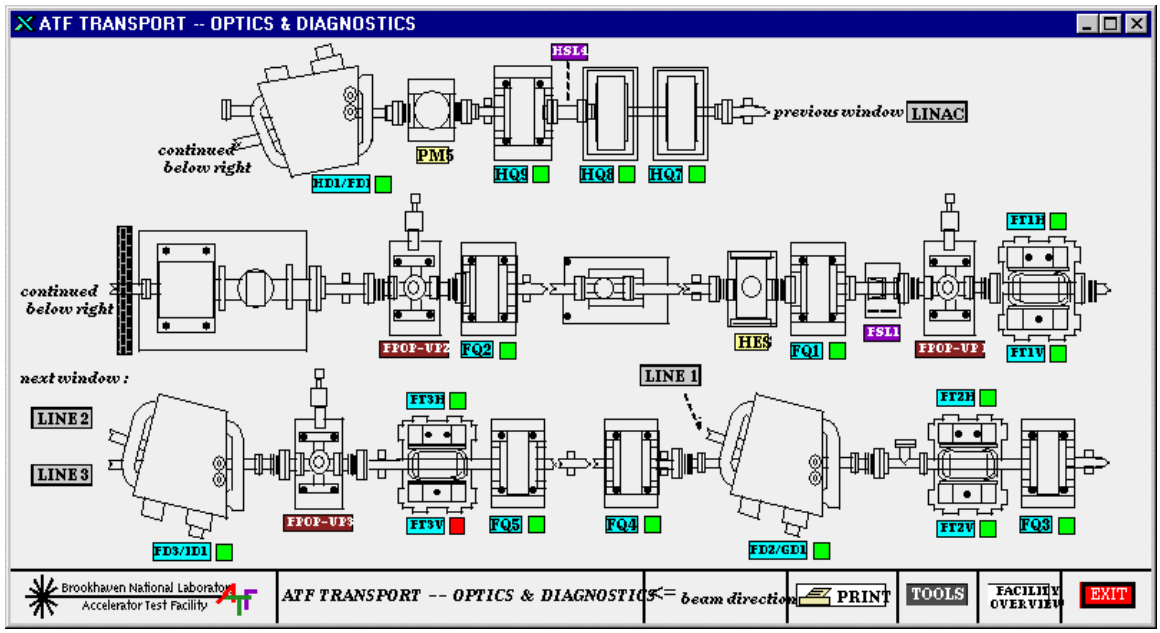

Figure 3-11 Control-computer display showing elements of the ATF H and F Transport Line

3.6 The I Line (BEAM-LINE 2)

The electron beam is transported to the experiment hall through the F line. At the Experiment Hall the beam may be sent to any one of three beam lines. The experiment described below is running on beam line number 2 (BL2). In order to get the beam to BL2 we turn off dipole FD2 (which sends the beam into BL1 when energized). As shown in Figure 3-11 we have various quadrupoles and steering magnets to adjust the beam optics and steer the beam to the correct trajectory.

To direct the beam into BL2, we energize dipole magnet (FD3) which bends the beam -20^{0} back to the original direction. With that, and proper settings of the F line quadrupoles, we can make BL2 dispersion-free. At present, BL2 has three important insertion devices: the Modulator, the Dispersion Section and the Radiator [16].

In addition to the electron beam, BL2 has a zinc selenide input window located in FD3 to inject a laser beam into the beam line. The laser beam can be aligned to overlap with the electron beam in the Modulator.

The Modulator is a variable gap permanent magnet wiggler. Its parameters are shown in Table 3-2.

modulator length	m	0.76
λ (Radiation wavelength)	nm	10600
λ_w (Wiggler period) (used)	cm	8
k_w (Wiggler wave number)	cm^{-1}	0.785
G_w (Wiggler gap)	cm	variable
B_w (Wiggler peak field)(used)	Tesla	0.16
K (Wiggler parameter, peak, used)		1.2

Table 3-2 Modulator parameters

The trajectory of the electrons in the modulator is shown in Figure 3-12. There is 0.5 mm horizontal offset in the trajectory. In order to place the electron beam trajectory in the correct place in the Modulator and to overlap the beam with the seed laser, we have a few diagnostic devices. We have one pop-in monitor before the modulator (IPOP-UP 1), one in the middle of the modulator (IPOP-UP 1.5) and one after the modulator (IPOP-UP 2).

The seed laser in use in this experiment is a CO_2 laser. Its interaction with the electron beam in the Modulator creates an energy modulation in the beam (See Figure 2.2-4).

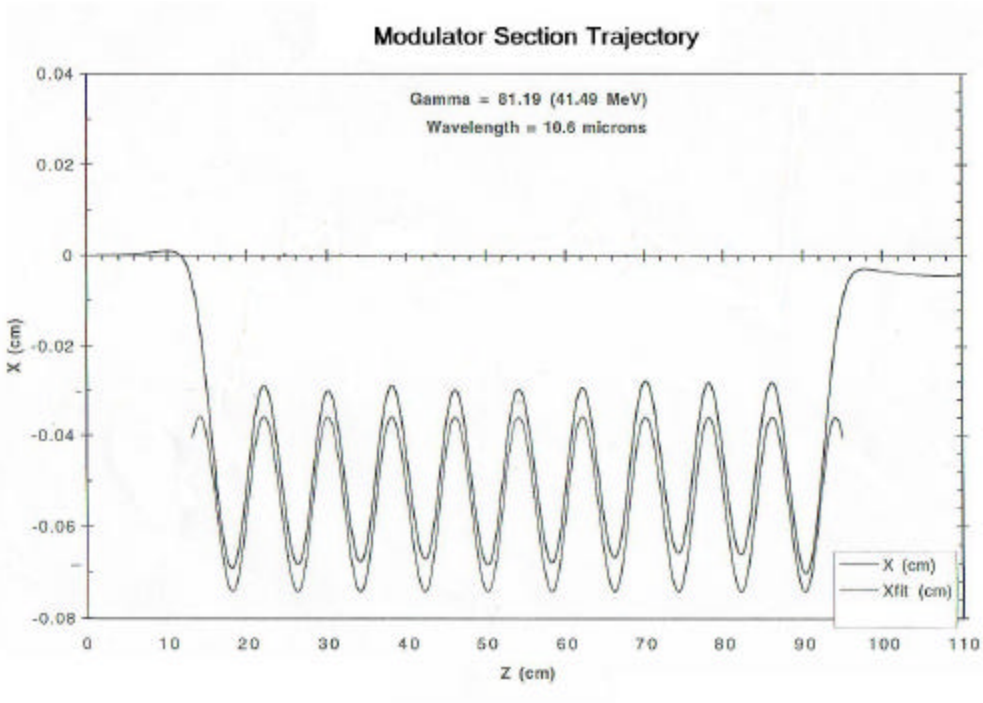

Figure 3-12 Wiggle-plane electron trajectory in the Modulator Section

The next important element is the dispersion magnet. The dispersion magnet basically consists of three dipole magnets as shown in Figure 3-13.

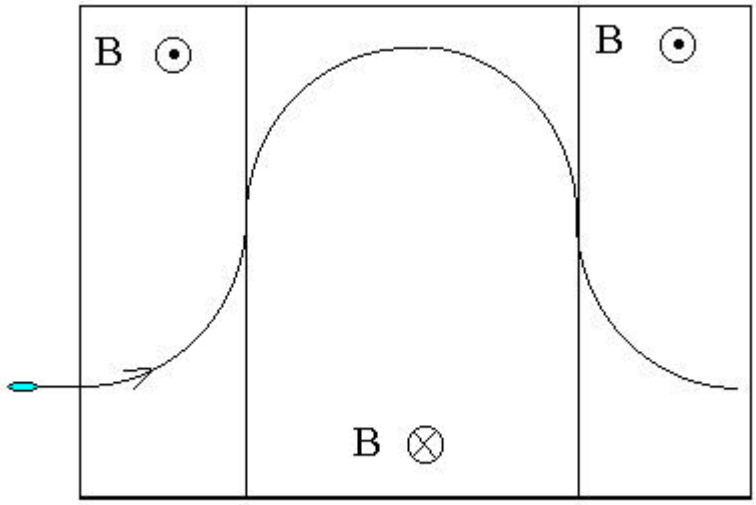

Figure 3-13 The electron trajectory in the dispersion magnet

The reference electron trajectory in the dispersion magnet is also shown in Figure 3-13. Higher energy electrons bend less than the reference electrons and vice versa. As mentioned above, the electron energy was modulated in the modulator by the seed radiation. In the dispersion section the more energetic electrons catch up with less energetic electrons, producing a larger concentration of electrons in a particular phase. This process is the 'micro bunching' described in section 2.2.

The last important element is the Radiator. The parameters of the Radiator wiggler are shown in Table 3-3. In the Radiator the electrons wiggle in horizontal direction and the axis is offset to the right by 700 micron. There are four electromagnets overlapping the permanent magnet wiggler to provide steering and extra focusing to equalize the horizontal and vertical focusing strength (wiggler's natural focusing is just in the vertical plane).

wiggler length	m	2
λ (Radiation wavelength)	nm	5000
λ_w (Wiggler period) (used)	cm	3.3
k_w (Wiggler wave number)	cm^{-1}	1.9
G_w (Wiggler gap)	cm	1.416
B_w (Wiggler peak field)(used)	Tesla	0.485
K (Wiggler parameter, peak)		1.495

Table 3-3 Radiator wiggler parameters

In the Radiator wiggler we have five pop-in monitors to observe the electron beam. The alignment of the electron beam is facilitated by a helium-neon laser (He-Ne laser), which defines the beam axis.

After exiting the radiator wiggler the beam is bent to the right by a dipole magnet designated as ID-2, thus separating the electron beam from the radiation. This dipole also serves as an energy spectrometer thus we can correlate the horizontal beam size to the energy spread in the beam. At the end of the beam line the beam is dumped in a radiation-shielded Faraday cup. At that location there is also the IPOP-UP 3 diagnostic. Using this monitor we can see the energy modulation of the beam due to the interaction with the radiation (CO_2 Laser). By retracting this monitor it is possible to measure the charge using the Faraday cup.

The electromagnetic radiation produced by the wiggler exits the beam line after the dipole magnet through a zinc selenide window and transported to the FEL room to be analyzed. The transport line for radiation will be described in the next chapter.

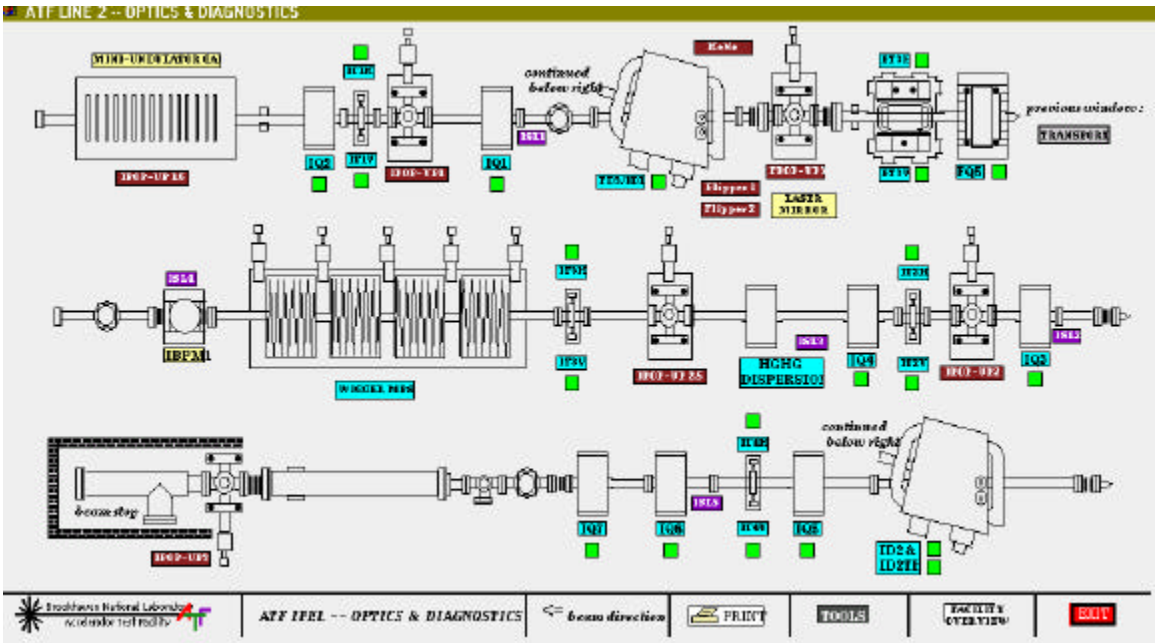

Figure 3-14 Control-computer display showing elements of the Beam-line2 electron beam transport line